


CEBAF-PR-85-003 VWC3  
Franz Gross  
Electromagnetic Stu\ In Nuclei  
\* 020592000094004  
  
80205920000940048

CEBAF 85-003

# ELECTROMAGNETIC STUDIES IN NUCLEI

Franz Gross  
Continuous Electron Beam Accelerator Facility  
12070 Jefferson Avenue  
Newport News, Virginia 23606

Invited talk presented at the "International Conference on Hadronic Probes and Nuclear Interactions", Arizona State University, Tempe, Arizona, 11-14 March 1985. To be published in the proceedings.

## ELECTROMAGNETIC STUDIES IN NUCLEI

Franz Gross  
Continuous Electron Beam Accelerator Facility  
12070 Jefferson Avenue  
Newport News, Virginia 23606

### ABSTRACT

This talk is devoted to a brief review of the experimental program for the new generation of multi GeV continuous beam electron accelerator facilities. First, the kinematic variables used in electron scattering are reviewed, three experiments which are representative of previous work in this field are described, and some comparisons are made between electron and hadronic probes. The main part of the talk then describes seven experiments proposed for the future. These are concerned with the structure of light nuclei, the structure of mesons and baryons, the influence of the nuclear medium on hadronic interactions, and the weak interactions.

### INTRODUCTION

Most previous work in nuclear physics with electrons, at least in the region of energy from several hundred MeV to several GeV, has involved the use of pulsed beams. Usually in this situation only one of the particles in the final state is detected, and this is normally the scattered electron. When the scattering is elastic, the quantity which is measured is referred to as the form factor, and its Fourier transform is usually interpreted as the charge or magnetic moment distribution of the target nucleus. Transition form factors, in which the scattering is to a definite final state not identical to the initial nuclear state, have also been measured and programs of such measurements have enabled us to learn a great deal about nuclear shell structure. When the scattering is to the nuclear continuum, the quantities measured are referred to as structure functions, and their study gives us important information about nuclear excitations and the degrees of freedom which are important in nuclear structure.

The new generation of electron accelerators, such as the 4 GeV Continuous Electron Beam Accelerator Facility (CEBAF) and the 1 GeV Bates-MIT proposal, will provide a continuous electron beam. This will make it possible to make measurements in which both the scattered electron and hadronic particles from the shattered nucleus are measured in coincidence. As I will describe below, coincidence experiments give information about many new quantities such as single particle densities and two-body correlations.

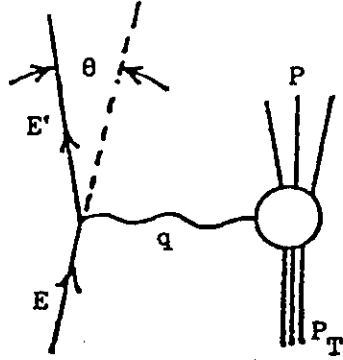


Fig. 1. Kinematics of single arm electron scattering.

The kinematics for single-arm measurements in which only the scattered electron is detected are shown in Fig. 1. There are three variables: the energies of the incoming and outgoing electrons ( $E$  and  $E'$ ), and the laboratory scattering angle  $\theta$ . Only two combinations of these three variables are needed to describe the unknown strong vertex; the dependence on the third variable,  $\theta$ , is given by the electromagnetic interaction with the point-like electron, which is known exactly. One of these two hadronic variables is  $Q^2$ , the square of the 4 momentum transferred by the electron,

$$Q^2 = -q^2 = 4EE'\sin^2\theta/2 \quad (1)$$

and the other is either  $\nu$ , the energy lost by the electron in the laboratory system, or  $W^2$ , the square of the invariant mass of the final hadronic state

$$\nu = \frac{q \cdot P_T}{M_T} = E - E'$$

$$W^2 = P^2 = M_T^2 - Q^2 + 2M_T\nu \quad (2)$$

where  $M_T$  is the target mass. If the scattering is to a definite final state with a fixed mass  $W^2 = M^{*2}$ , then the hadronic part of the cross section depends only on one variable,  $Q^2$ .

When the scattering is elastic, so that the nucleus remains in its ground state, the differential cross section is given by

$$\frac{d\sigma}{d\Omega} = \sigma_M\left(\frac{E'}{E}\right) [A(Q^2) + B(Q^2)\tan^2 \frac{\theta}{2}] \quad (3)$$

where the scale is set by the Mott cross section

$$\sigma_M = \left(\frac{\alpha}{2E}\right)^2 \frac{\cos^2(\frac{1}{2}\theta)}{\sin^4(\frac{1}{2}\theta)} \quad (4)$$

where  $\alpha$  is the fine structure constant. For inelastic scattering it is customary to define the doubly differential cross section

$$\frac{d^2\sigma}{d\Omega dE'} = \sigma_M [W_2(Q^2, \nu) + 2W_1(Q^2, \nu)\tan^2 \frac{\theta}{2}] \quad (5)$$

where  $W_1$  and  $W_2$  are the structure functions which contain all the hadronic information.

Figure 2 gives some feeling for how a typical structure function depends on the two variables  $\nu$  and  $Q^2$ . Note that when the momentum transfer  $Q$  is non-zero, but is much smaller than the inverse of the nuclear radius,  $R$ , the principle features of the excitation spectrum are elastic scattering and excitation of the giant resonances. As  $Q$  is increased, the elastic peak moves according to the relation

$$\nu = \frac{Q^2}{2M_{\text{nucleus}}} \quad (6)$$

and higher lying states of the nucleus are more strongly excited. Finally, when the momentum transfer is much larger than the inverse

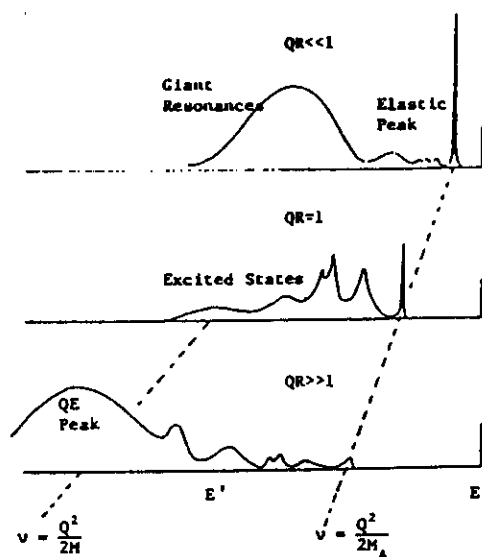


Fig. 2. A typical excitation function for electron scattering for three different regions of  $Q$ .

of the nuclear radius, transitions in which the final nucleus is in its ground state or a low-lying excited state become suppressed, and the major feature is quasi-elastic scattering from the individual nucleons in the nucleus. As shown below, in Fig. 6, at much higher  $Q^2$  even quasi-elastic scattering becomes suppressed and one sees the scattering from individual quarks which make up nuclear matter.

Figure 2 shows that by varying  $Q^2$  and  $\nu$ , a wide variety of nuclear phenomena can be studied. Elastic scattering, which fixes  $\nu$  according to Eq. (6), gives us the elastic form factor of the nuclear ground state. For a spin zero target, such as  $^{40}\text{Ca}$ , the structure function  $A(Q^2)$  is equal to

the square of the nuclear form factor,  $F(Q)$ . If relativistic effects are ignored, then the form factor can be related directly to the nuclear charge distribution by

$$\rho(r) = \int_0^\infty Q^2 dQ j_0\left(\frac{Qr}{2}\right) F(Q) \quad (7)$$

where  $j_0$  is the spherical vessel function of order 0 and the factors of  $\pi$  have been omitted. Figure 3, taken from an old conference talk by Sick<sup>1</sup>, shows the world's data on elastic scattering from  $^{40}\text{Ca}$ . These measurements, which in this case extend over 12 orders of magnitude, are typical of the high precision which can be attained with electron scattering. The numerical Fourier transform of the data leads to the charge distribution shown in Fig. 4, which also

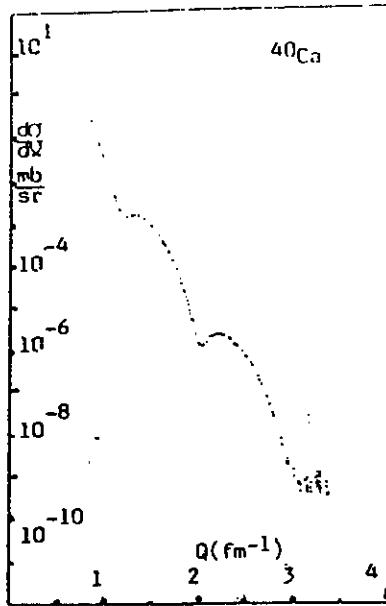


Fig. 3. The differential cross section for electron scattering from  $^{40}\text{Ca}$ .

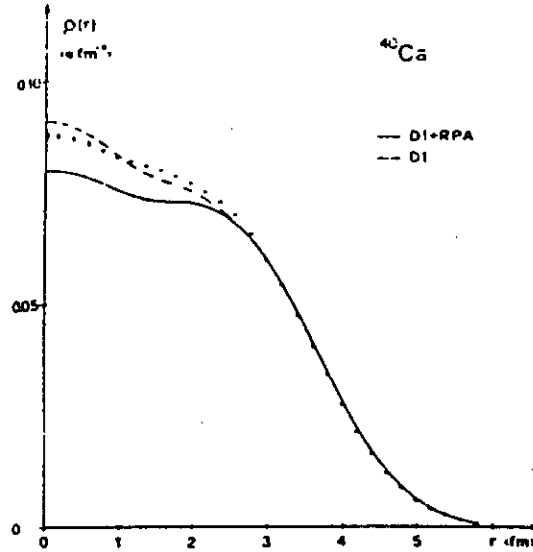


Fig. 4. Two theoretical charge distributions compared with the model independent result obtained from Eq. (7).

includes a comparison with two theoretical calculations. This sort of comparison between theory and experiment has been carried out on a large number of nuclei, and is an important source of our theoretical understanding of nuclear structure.

By letting  $\nu$  be slightly larger than the value given by Eq. (6), it is possible to probe transitions to low-lying excited states. Figure 5, taken from reference 2, illustrates this class of measurements. In this example, the final pn system has a center of mass energy in the range from 0 to 3 MeV, so the electromagnetic transition is from the initial deuteron to a final state which is largely  $^1S_0$ . As the curves show in the figure, this measurement is famous for showing that the non-relativistic impulse approximation fails completely, and that meson exchange or relativistic effects are essential for explaining the data. The recent data is at  $Q^2$  sufficiently high so that details of the meson exchange effects can be studied. An extensive program of measurements of this kind on nuclei throughout the periodic table has been carried out at Bates.

As a final example of single arm electron scattering, the proton structure function  $\nu W_2$  measured at SLAC in the early 1970's is shown in Fig. 6, taken from the Barnes Committee Report<sup>3</sup>. Here the structure function is plotted as a function of the two variables,  $Q^2$ , and a dimensionless scaling variable,  $\omega'$ , obtained from the ratio of  $W^2/Q^2$ . The figure shows clearly the electromagnetic excitation of three nucleon resonances: the  $\Delta(1232)$ ,  $N_1^*$  ( $\approx 1500$ ) and  $N_2^*$  ( $\approx 1650$ ).

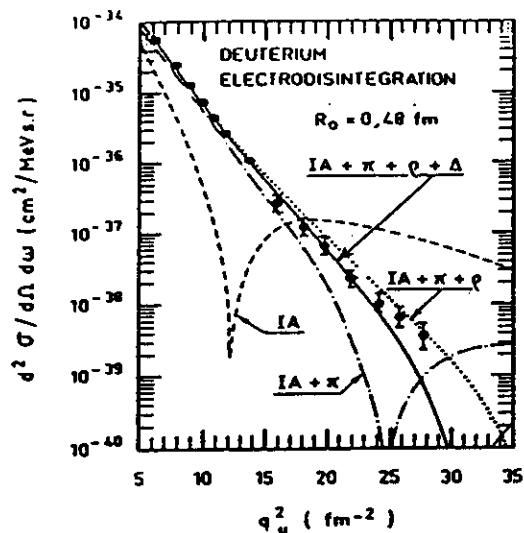


Fig. 5. Differential cross section for  $D(e, e')pn$ . The dashed line labeled IA is the non-relativistic impulse approximation; the others include various meson exchange contributions.

The dashed line just above the  $N_2^*$  peak is the line with fixed  $W=2$  GeV. Above this boundary, individual resonances begin to disappear and the structure function assumes a featureless shape which becomes a universal function of the scaling variable  $\omega'$ , independent of  $Q^2$ . This lack of dependence on  $Q^2$  tells us that the electrons in this region are scattering from the point-like quark constituents, and it follows that the disappearance of the resonance peaks and the emergence of the smooth scaling behavior is a signal of the transition from a region where the physics is dominated by collective quark degrees of freedom (or excited baryon and meson clusters) to one where individual quark degrees of freedom emerge as the

dominant effect. Fig. 7 shows that this entire transition region can be studied with a 4 GeV electron accelerator, and is one of the principle reasons for selection of 4 GeV for the energy of the CEBAF project.

I will return to a discussion of programs proposed for the new generation of continuous beam electron accelerators in a moment. I now turn briefly to another topic.

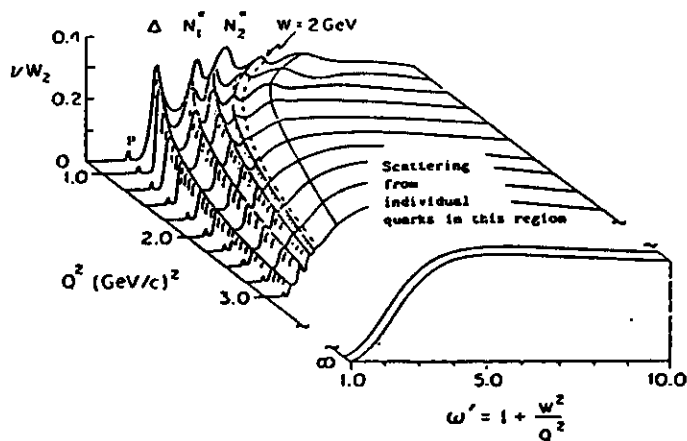


Fig. 6. The proton inelastic structure function  $\nu W_2$  shown as a function of  $Q^2$  and the scaling variable  $\omega'$ .

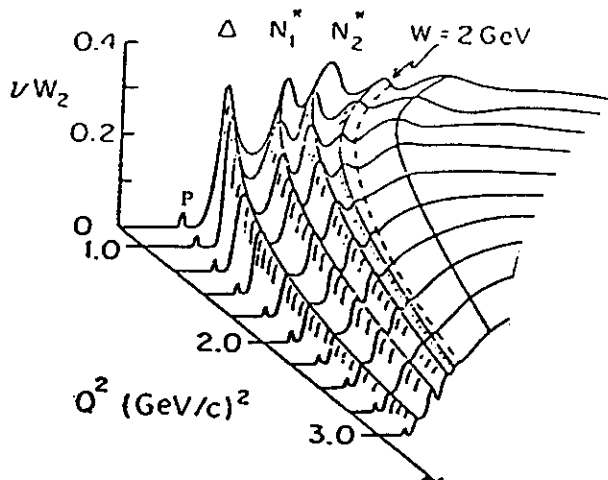


Fig. 7. The part of the surface shown in Fig. 6 which is accessible with 4 GeV electrons.

### COMPARISON WITH HADRONIC PROBES

Perhaps the most striking difference between the electron and hadron probes is that the electromagnetic interaction is much weaker than the strong interaction. The fine structure constant is two orders of magnitude smaller than typical meson-baryon coupling constants, and at least one order of magnitude smaller than the quark gluon coupling constant in the region of momentum transfers relevant to nuclear physics experiments. One of the major consequences of this fact is that the interaction of the electron with the nucleus is basically perturbative in the sense that it is sufficient to treat the electron-nucleus interaction in the one-photon exchange approximation, as shown in Fig. 8. (For nuclei with large  $Z$ , one uses distorted waves for the initial and final electron, which takes into account the major effects of the higher order Coulomb interactions.) The situation with hadronic probes is, of course, quite different; nobody would dream of treating the proton-nucleus interaction in the one-pion exchange approximation as shown also in Fig. 8. One of the

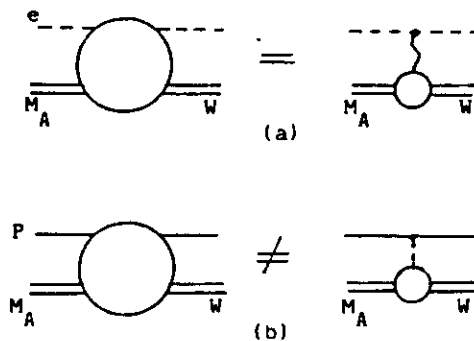


Fig. 8. (a) Electron nucleus and (b) proton nucleus scattering diagrams.

consequences of this difference between electron and proton scattering is that the dependence of the total amplitude on the Mandelstam variable  $s$  is known in electron scattering; the hadronic interaction depends non-trivially on three variables  $s$ ,  $t = -Q^2$  and  $W^2$ , whereas the electron scattering amplitude depends on only two of these. The separation into longitudinal and transverse parts, which is so commonly discussed in electron scattering, has no direct analog in reactions involving hadronic probes.

Another consequence of the fact that the electron interacts weakly with nuclei, which is not an advantage, is that the counting rates in electron scattering experiments are very low.

There are several other differences between electrons and hadrons as probes, which are a consequence of the fundamental difference between electrons and quarks. The electron is fundamentally different from a proton or a pion, and retains its identity throughout the interaction. This means that one does not need to anti-symmetrize the amplitudes as in the case with proton probes. At the most fundamental level, the electron interacts only with charged particles; it sees quarks only and does not interact directly with gluons. The quark, which is the constituent of all hadronic probes, interacts both with quarks and gluons as illustrated in Fig. 9. Unfortunately, neither interaction is very simple because of higher order effects which cannot be neglected at the momentum transfers one encounters in nuclear physics. Because of these fundamental differences between electron-nucleus and hadron-nucleus interactions, it is important that the nuclear physics community have a variety of probes available for the study of the nucleus. Electrons "see" quarks only, while hadrons "see" both quarks and gluons, so they are truly complementary probes.

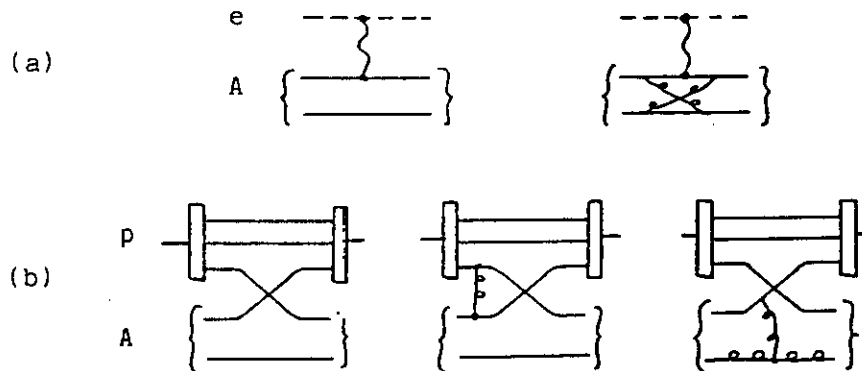


Fig. 9. (a) Electron nucleus and (b) proton nucleus scattering diagrams at the quark level.

#### PROPOSED PHYSICS PROGRAM

I now turn to a brief overview of the physics program currently planned for the new generation of high energy high duty factor electron accelerators<sup>4,5</sup>. I will focus principally on the program planned for CEBAF, although a fraction of this program could also be carried out with the lower energy project planned at Bates. The CEBAF program is continually under review by user working groups<sup>6</sup> and will certainly evolve before the accelerator is finished in 1991 or 1992.

The specific experimental programs proposed fall into four major categories:



- (i). Structure of Light Nuclei - including measurements of wave functions, study of the role of color degrees of freedom, and, for example, separation of the deuteron monopole and quadrupole form factors.
- (ii). Structure of Mesons and Baryons - including measurements of the kaon and neutron form factors, and study of the vector mesons and excited baryons.
- (iii). Influence of the Nuclear Medium on Hadronic Interactions - including study of the  $\Delta$  propagation through a nuclear medium, NN correlations through the  $(e, e'NN)$  reaction, production of hypernuclei by the  $(\gamma, K)$  reaction, and influence of the nuclear medium on the hadronization of quarks.
- (iv). Weak Interactions - including study of parity violating effects in  $eN$  scattering and use of nuclei to test the standard model.

The long range goal of the CEBAF is to study the clustering of quarks in the nuclear medium, the role of color degrees of freedom in nuclei, and non-perturbative aspects of QCD.

#### 1. Structure of Light Nuclei

I will begin with a typical coincidence experiment in which two particles in the final state, the scattered electron and an outgoing nucleon, are measured simultaneously. Such  $(e, e'N)$  measurements contain important new information not obtainable from single arm measurements. If meson exchange effects or final state interactions are small, the electromagnetic interaction could be calculated from the diagram shown in Fig. 10. The triply differential cross section obtained from this diagram is given by

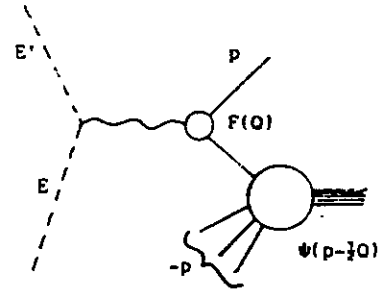


Fig. 10. The simplest Feynman diagram describing  $(e, e'p)$  scattering.

$$\frac{d^3\sigma}{d\Omega dE' d\vec{p}} = \sigma_M |F(Q)|^2 |\psi(p - \frac{1}{2} Q)|^2 \quad (8)$$

where, as usual, the scale of the overall cross section is set by the Mott cross section,  $F(Q)$  is the form factor of the nuclear constituent, and  $\psi(p - \frac{1}{2} Q)$  is the relativistic wave function of the struck nucleon. The wave function depends on the relative momentum of the struck nucleon with respect to the other nuclear constituents, and,

as can be seen from Fig. 10, is related to the covariant vertex function in which the struck nucleon is off-shell and the other nucleons and the initial nuclear system are on-shell. Eq. (8) shows us, therefore, that such measurements can in principle give us a direct measurement of the square of the relativistic wave function. (In practice, of course, final state interactions and meson exchange effects introduce corrections to this simple picture which may be significant.)

For comparison, the same simple theory gives the following expression for the single arm cross section

$$\frac{d^2\sigma}{d\Omega dE'} \approx \sum_{\beta} \sigma_M |F_{\beta}(Q)|^2 \int d^2\hat{p} |\psi_{\beta}(p - \frac{1}{2}Q)|^2 \quad (9)$$

This expression differs from Eq. (8) in two important respects. First, the direction of the momentum of the final struck particle is integrated over, which means that the expression will always be dominated by that part of the phase space where the relativistic wave function has a maximum, making it difficult to measure the wave function in regions where it is small. A second difference is the sum over  $\beta$ , where  $\beta$  labels the different Fock space components of the wave function. In cases where we wish to study a particularly small Fock space component, such as the  $\Delta\Delta$  contribution to the deuteron, it

is a distinct advantage to be able to look at the final hadronic particles and use them as a means to select against the larger Fock components.

A program of such measurements has already been started at Saclay. Fig. 11, taken from reference 7, shows the results of  $(e, e'p)$  measurements from the deuteron. I have added to the figure a curve which shows roughly how the momentum distribution would fall if the deuteron had only an S state; clearly, the data is very sensitive to the D state component which in turn is a measure of the strength of the tensor force.

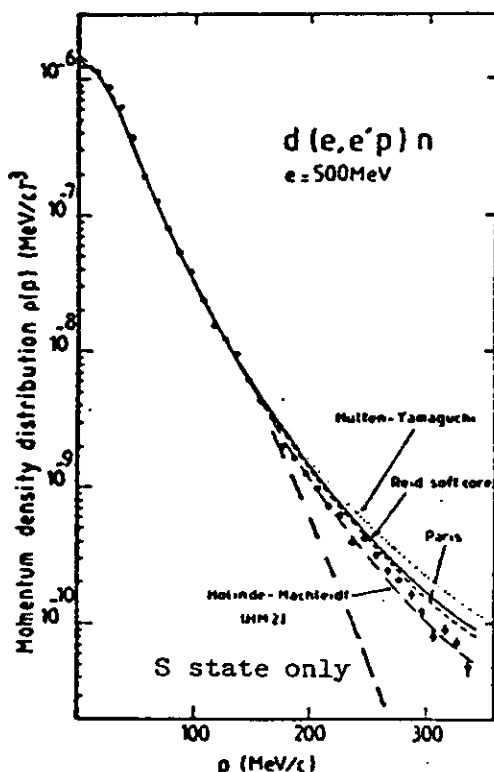


Fig. 11. Deuteron momentum density as extracted from the Saclay coincidence experiment. The D state probability of the models shown is HY (7%), RSC (6.5%), Paris (5.46%), and HM (4.32%).

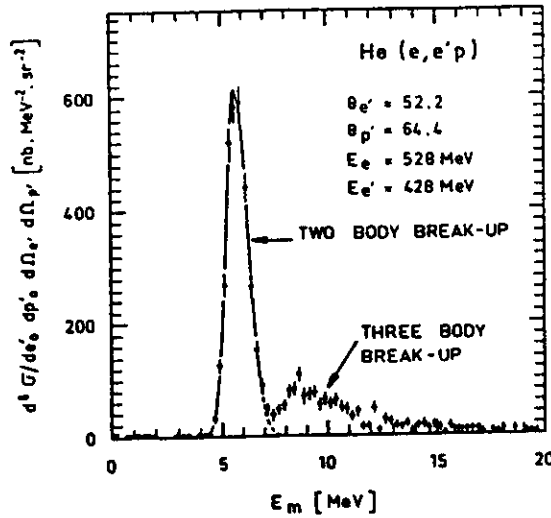


Fig. 12. Separation of the 2- and 3-body final state by missing energy.

Similar results have been obtained for the 3-body system from Saclay  $^3\text{He}(e, e'p)d$  and  $^3\text{He}(e, e'p)np$  data<sup>8</sup>. Fig. 12, taken from reference 8, shows how the 2- and 3-body contributions can be separated from one another, and Fig. 13 shows the momentum space dependence of each of these separate Fock components. At CEBAF we will be able to extend these measurements to much higher momentum transfer, and to study more exotic processes.

An example of such an exotic process is the  $N^*(1688)p$  component of the deuteron wave function<sup>9</sup>. The idea here is to separate the pre-existing  $N^*p$  component of the deuteron wave function, shown in Fig. 14a, from other contributions which

could give rise to the same final state. These are photo-production of the  $N^*$ , shown in Fig. 14b, and production of the  $N^*$  in a final state interaction, shown in Fig. 14c. With a 4 GeV CW electron accelerator, one has sufficient energy to choose the kinematics so

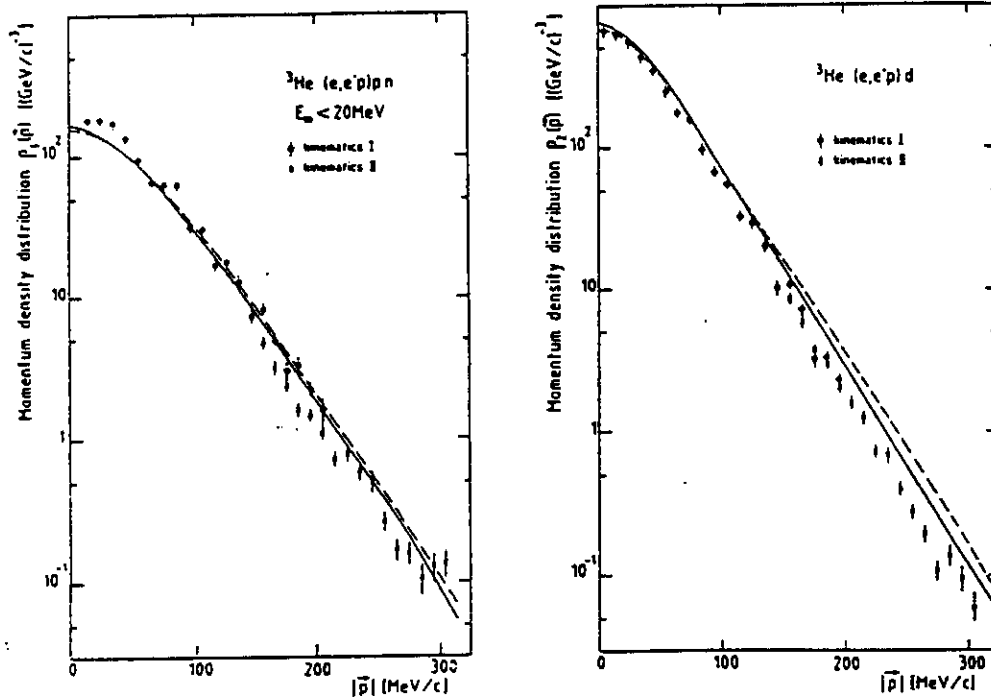


Fig. 13. Momentum density distributions for (a) the 2-body, and (b) the 3-body sectors in inelastic electron scattering from  $^3\text{He}$ .

that the momentum of the spectator nucleon cannot be less than 350 MeV/c and that the kinetic energy of the final state  $N^*p$  system is bigger than 175 MeV. The first condition ensures that the  $N^*$  wave function is comparable to the D state component of the deuteron, both of which tend to peak in the vicinity of 350 MeV/c and are larger than the S state wave function at these high momenta. The second condition ensures that final state interactions will be kept to a minimum. In reference 9 it was found that pre-existing  $N^*p$  components as large as 0.1% could be measured in this way.

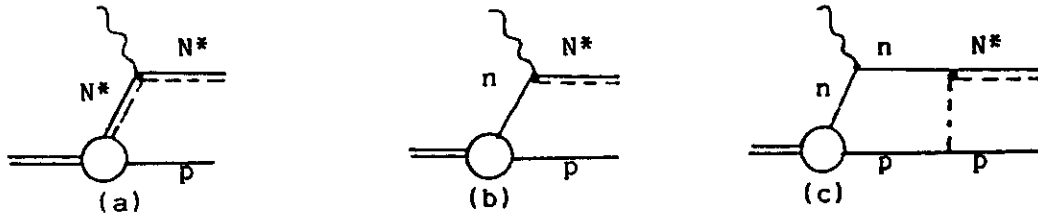


Fig. 14. Feynman diagrams for (a) knockout of a pre-existing  $N^*$ , (b) electro-production of the  $N^*$ , and (c) production of the  $N^*$  by final state interactions.

As a last example of measurements involving the structure of light nuclei, I discuss the deuteron form factors. The deuteron, being a spin 1 system, has three form factors: the electric monopole  $G_C$ , the electric quadrupole  $G_Q$ , and the magnetic  $G_M$  form factors. Single arm measurements with unpolarized particles can measure only two combinations of these three quantities

$$\begin{aligned} A(Q^2) &= G_C^2 + \frac{8}{9}\eta^2 G_Q^2 + \frac{2}{3}\eta G_M^2 \\ B(Q^2) &= \frac{4}{3}\eta(1+\eta)G_M^2 \end{aligned} \quad \eta = \frac{Q^2}{4M_d^2} \quad (10)$$

The A structure function was measured to high  $Q^2$  some time ago and the B structure function has recently been measured at Saclay, and will soon be measured to high  $Q^2$  by the new NPAS facility at SLAC.

To separate  $G_C$  and  $G_Q$  from one another requires some spin measurement; one way is to carry out a polarization transfer measurement in which the polarization of the electron is transferred to the recoiling deuteron whose polarization is measured in a second, analyzing scattering<sup>10</sup>. A second, equivalent, method is to scatter polarized electrons from a polarized deuteron target. The first method requires the construction of a deuteron polarimeter, and is much more easily carried out on a high duty factor accelerator. Since it is

difficult to maintain the polarization of the target in the presence of the intense electron beams required for these measurements at high  $Q^2$ , the second measurement probably requires the construction of an internal target facility, in which a circulating electron beam of very high current interacts with a gas jet of polarized deuterons. Both Bates and CEBAF will have stretcher rings which are necessary for the construction of such a facility.

## 2. Structure of Mesons and Baryons

A program of photo-production of excited baryons and a proposal to measure the electric form factor of the neutron will be discussed in this section.

The spectrum of mesons and baryons continues to be a fundamental testing ground for non-perturbative QCD. On the whole, simple quark models do a very good job describing the spectrum of baryons, but in the mass region around 2 GeV a number of states are predicted that are not seen in  $\pi$ -nucleon scattering. One reason for this, which is also suggested by the models themselves, is that such states may not couple significantly to the  $\pi N$  channel; they may decay predominantly into such channels as  $\Delta\pi$ ,  $N\rho$ , and  $N\gamma$ . In such cases we could expect to photo-produce these states and observe their decay into the  $N\pi\pi$  channel. Specific examples<sup>11</sup> of such states which are expected to behave this way are the  $F_{15}(1955)$ ,  $P_{13}(1955)$ ,  $F_{15}(2025)$ , and the  $F_{35}(1975)$ . Experiments to study these states using a tagged photon beam and a Large Acceptance Detector (LAD), which would detect most of the final state particles, appear to be feasible.

The neutron electric charge form factor,  $G_{En}$ , is one of the fundamental quantities in physics and is very poorly known; the low  $Q^2$  data has large statistical errors and large unknown systematic errors and there is no data at  $Q^2$  greater than  $1(\text{GeV}/c)^2$ . This is

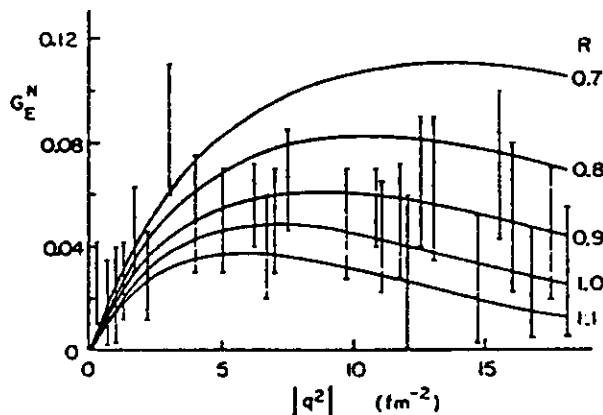


Fig. 15. Data on  $G_{En}$  compared to predictions from quark bag models with different radii.

particularly serious because a knowledge of  $G_{En}$  is needed before one can extract information about nuclear structure from high  $Q^2$  measurements on simple nuclei. Fig. 15, from reference 12, shows that  $G_{En}$  is also sensitive to quark model parameters.

Straight forward measurement of  $G_{En}$  by Rosenbluth separation is very difficult because its contribution to

the A structure function enters as  $G_E^2 + \tau G_M^2$ ,  $\tau = \frac{Q^2}{4M^2}$ , where it

is always dwarfed by the magnetic form factor. The best way to measure  $G_E$  is with a spin measurement; either a polarization transfer measurement in which the electron polarization is transferred to the recoiling neutron<sup>10</sup> or a spin correlation experiment in which the polarized electron scatters from a polarized neutron (i.e., deuteron) target. In the former case the double scattering cross section is given by

$$\frac{d^2\sigma}{d\Omega d\Omega_2} = \frac{d^2\sigma}{d\Omega d\Omega_2} \Big|_0 \{1 + a p_x A_y \sin\phi_2\} \quad (11)$$

where  $a$  is the polarization of the electron,  $A_y$  is the analyzing power of the secondary scattering, and  $\phi_2$  is the azimuthal angle through which the neutron is scattered. The polarization transfer coefficient  $p_x$  is proportional to the product of  $G_E G_M$

$$I_0 p_x = I_0 K_{LS} = -2\tau(1+\tau)G_E G_M \tan\left(\frac{1}{2}\theta\right) \quad (12)$$

where  $I_0$  is proportional to the unpolarized cross section. These experiments are very difficult, but they have the advantage of giving a signal directly proportional to  $G_E$ .

### 3. Influence of the Nuclear Medium on Hadronic Interactions

While electron energies as high as 1 GeV are not required for many experiments which probe the structure of heavy nuclei, there are some very important classes of measurements which require energy in excess of 2 GeV. Two such measurements, which look very promising, will be described.

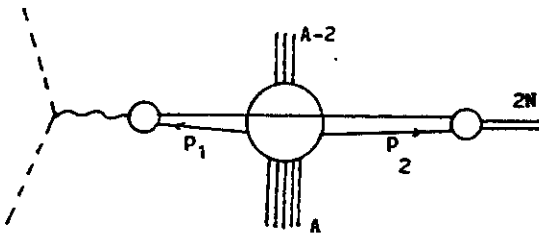


Fig. 16. Simplest Feynman diagram for knockout of two colinear nucleons.

Two nucleon knockout, through the process  $(e, e'2N)$  appears to be a very promising way of studying nucleon-nucleon correlations. Several kinematic configurations can be devised for observing the two outgoing nucleons. In one case<sup>13</sup>, the two nucleons come out parallel to each other, and are detected in a single spectrometer. If the two outgoing nucleons have a large momentum with respect to the rest of the nucleons in the nucleus, final state interactions will be reduced, and one hopes that the process will be

dominated by the diagram shown in Fig. 16. The multiply differential cross section obtained from this simple diagram is proportional to the probability that the two nucleons detected in the final state

had initial momentum  $p_1$  and  $p_2$ . If  $p = \frac{1}{2}(p_1 - p_2)$  is the relative momentum between these two nucleons, then the cross section is directly proportional to the square of the momentum space correlation function, which is a function of the quantity  $p$ . Initial estimates suggest that these measurements require electron energy in excess of 3 GeV, high duty factor and intense beams.

Another program which looks very promising for the study of nuclear structure is the production of hypernuclei by the  $(\gamma, K)$  reaction<sup>14</sup>. Figure 17a shows the basic process by which the hypernucleus

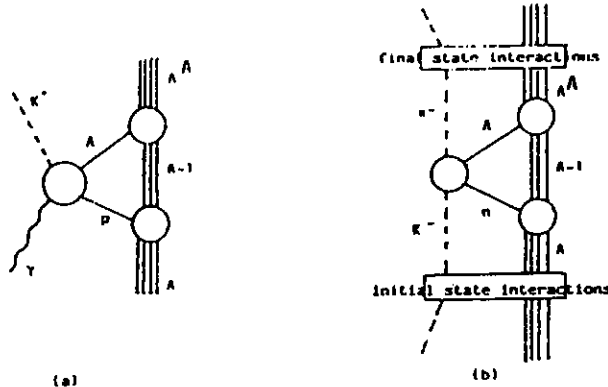


Fig. 17. (a) Elementary mechanism for the production of hypernuclei by the  $(\gamma, K)$  reaction. (b) Similar diagram for the production of hypernuclei by the  $(K^-, \pi^-)$  reaction.

is formed. This is to be compared with the process by which hypernuclei are formed using  $K^-$  beams, shown in Fig. 17b. One of the advantages which the  $(\gamma, K)$  reaction has over the conventional  $(K^-, \pi^-)$  reaction is that both the photon and the  $K^+$  are very weakly interacting particles, so that the initial and final state interactions

tend to be fairly small and can be regarded as corrections to the basic process, Fig. 17a. This is not the case for the  $(K^-, \pi^-)$  reaction, where initial and final state interactions are very large because both the  $K^-$  and the  $\pi^-$  interact strongly. T. W. Donnelly, who has popularized these studies, likes to emphasize the fact that the strong interactions of the  $K^-$  and  $\pi^-$  probes would make it impossible to deposit a  $\Lambda$  particle in the center of lead, whereas this can be done with photons. Another difference between the  $(\gamma, K)$  reaction and the  $(K^-, \pi^-)$  reaction is that the former will excite both unnatural and natural parity states, whereas the latter will strongly excite only natural parity states. This program would be an exciting, totally new way to study hypernuclei, but it represents a very serious challenge to those building the experimental equipment. High resolution spectrometers ( $\Delta p/p \approx 5 \times 10^{-5}$ ) are essential if the program is to achieve its maximum potential, and the short flight path of the kaon may pose special difficulties in the design.

#### 4. Weak Interactions

The study of parity violating effects in electron scattering is a good way to study the weak interactions. Any parity violating asymmetry, such as

$$A = \frac{\sigma_L - \sigma_R}{\sigma_L + \sigma_R} \quad (13)$$

where  $\sigma_L$  and  $\sigma_R$  are the total cross sections for left-handed and right-handed electrons, respectively, measures the interference between the one photon exchange diagram and the exchange of the  $Z^0$ . Since the one photon exchange diagram falls off as  $1/Q^2$ , while the  $Z^0$  diagram is approximately constant in  $Q^2$ , the asymmetry grows as  $Q^2$ . However, since the total cross section falls as  $Q^{-4}$ , the "figure of merit" for asymmetry measurements,  $A/\sigma$ , is independent of  $Q^2$ , so that the weak interference term can be studied over a wide range in  $Q^2$ . A number of interesting tests of the standard model have been proposed<sup>4,5</sup>.

Planning for the experimental program at CEBAF will be a continuing process for the next five or more years. The immediate activities we look forward to are the 1985 Summer Workshop, to be held from June 3-7, followed by a three month Summer Study Group which will meet at the Newport News site. Activities will continue through 1985-86, and more programs will be planned for the summer of 1986. The CEBAF management welcomes the participation of users from all sub-fields of nuclear physics; do not hesitate to join the users group and participate in these activities, even if you have never seen an electron before!



# REFERENCES

1. I. Sick, et al., Physics Lett. 88B, 245 (1979).
2. B. Frois, private communication.
3. The Role of Electromagnetic Interactions in Nuclear Science, an NSAC report (B. D. Barnes, Chairman - 1982).
4. See, for example, "Future Directions in Electromagnetic Nuclear Physics" (Workshop report, 1981).
5. See the SURA 1982 NEAL (CEBAF) proposal.
6. See the Proceedings of the CEBAF 1984 Summer Workshop, edited by F. Gross and R. R. Whitney, published by CEBAF, Newport News, Virginia.
7. M. Bernheim, et al., Nucl. Phys. A365, 349 (1981).
8. E. Jans, et al., Phys. Rev. Lett. 49, 974 (1982).
9. C. Perdrisat, et al., Mini-proposal #14 in Reference 5 and #12 in Reference 4.
10. R. Arnold, C. Carlson, and F. Gross, Phys Rev. C 23, 363 (1981).
11. R. Koniuk and N. Isgur, Phys. Rev. D 21, 1868 (1980) and N. Isgur, private communication.
12. S. Th  berge, G. A. Miller, A. W. Thomas, Can. J. of Phys. 60, 59 (1982).
13. J. W. Lightbody, Mini-proposal #16 in Reference 5 and #9 in Reference 4.
14. A. M. Bernstein, T. W. Donnelly, and G. N. Epstein, Mini-proposal #21 in References 4 and 5.